Nano@micro: General Method for Entrapment of Nanocrystals in Sol−Gel-Derived Composite Hydrophobic Silica Spheres

Taleb Mokari,[†,‡,§] Hanan Sertchook,[†,§] Assaf Aharoni,[†,‡,§] Yuval Ebenstein,[†,‡,§] David Avnir,*[,†,§] and Uri Banin*[,†,‡,§]

Institute of Chemistry, The Farkas Center for Light Induced Processes, and The Center for Nanoscience and Nanotechnology, The Hebrew University of Jerusalem, Jerusalem 91904, Israel

Received September 6, 2004. Revised Manuscript Received October 28, 2004

A general method for entrapment of hydrophobically coated nanocrystals in micrometer and submicrometer composite silica spheres, nano@micro, was developed. The method employs two starting solutions—hydrophobic solvent containing the sol−gel precursor, a polymer, and the nanocrystals, and an emulsifying hydrophilic phase which catalyzes the sol−gel process. The use of a hydrophobic polymer, polystyrene, serves to encapsulate the nanocrystals inside the spheres while maintaining many of their original properties. The obtained nano@micro spheres were characterized structurally by transmission electron microscopy and scanning electron microscopy, chemically by energy dispersive X-ray spectroscopy, and optically by ensemble and single-particle fluorescence spectroscopy. It is possible to control the size of the microspheres from the 100 nm scale to the micrometer scale, with good monodispersivity and with good separation between the microspheres. The method is demonstrated for encapsulating a wide variety of nanocrystals, primarily semiconductors covering different spectral bands, and of different shapes including spheres and rods. The semiconductor nanocrystals impart widely tunable emission to the microspheres. A similar encapsulation technique was also applied to thiol-coated Au particles. The technique is generally applicable to other hydrophobic nanocrystal systems of magnetic, oxide, and other materials.

Introduction

In recent years there has been major progress in methods for controlling the growth of nanocrystals (NCs) of semiconducting, metallic, magnetic, and oxide materials.[1] Shape control has enabled obtaining nanoparticles in forms such as dots, rods, tetrapods, and more.[2−6] The size-, composition-, and shape-dependent properties of such NCs can be harnessed for a variety of applications in areas ranging from biological fluorescent tagging[7,8] to light-emitting diodes,[9] lasers,[10,11] and catalysts.[12] Further development of applications of semiconductor NCs requires means for incorporating them in various matrixes. On one hand, this would provide protection and compatibility for the NCs with various environments, and on the other hand, this would impart specific properties of the NCs to the carrier matrix. Carrier matrixes which have drawn much attention in recent years are ceramic and oxide-glass sol−gel materials.

Earlier work on NCs in sol−gel materials focused primarily on hydrophilic, water-soluble NCs. For instance, CdS and PbS particles were prepared in aqueous solution and subsequently added to a sol.[13] Recently, additional types of water-soluble semiconductor NCs were entrapped in silica particles by a sol−gel process, forming "raisin bun"-type particles.[14] In a different strategy, sol−gel solutions were doped by cadmium ions and the resulting gels were heat treated in H_2S, forming CdS nanocrystals.[15] In yet another approach, thermal decomposition of sulfur-containing Cd^{2+} complexes was used.[16] However, these approaches are incompatible with high-quality NCs, which are typically covered with a hydrophobic coating. For these cases,

* To whom correspondence should be addressed. E-mail: banin@chem.ch.huji.ac.il (U.B.); david@chem.ch.huji.ac.il (D.A.).
† Institute of Chemistry.
‡ The Farkas Center for Light Induced Processes.
§ The Center for Nanoscience and Nanotechnology.

(1) *Nanoparticles—from theory to applications*; Schmid, G., Ed.; Wiley-VCH: New York, 2004.
(2) Peng, X. G.; Manna, L.; Yang, W. D.; Wickham, J.; Scher, E.; Kadavanich, A.; Alivisatos, A. P. *Nature* **2000**, *59*, 404.
(3) Kan, S. H.; Mokari, T.; Rothenberg, E.; Banin, U. *Nat. Mater.* **2003**, *2*, 155.
(4) Manna, L.; Milliron, D. J.; Meisel, A.; Scher, E.; Alivisatos, A. P. *Nat. Mater.* **2003**, *2*, 382.
(5) Jin, R.; Cao, Y.; Mirkin, C. A.; Kelly, K. L.; Schatz, G. C.; Zheng, J. G. *Science* **2001**, *294*, 1901.
(6) Dumestre, F.; Chaudret, B.; Amiens, C.; Renaud, P.; Fejes, P. *Science* **2004**, *303*, 821.
(7) Cao, Y. W. C.; Jin, R. C.; Mirkin, C. A. *Science* **2002**, *297*, 1536.
(8) Alivisatos, A. P. *Nat. Biotechnol.* **2004**, *22*, 47.
(9) Tessler, N.; Medvedev, V.; Kazes, M.; Kan, S. H.; Banin, U. *Science* **2002**, *295*, 1506.
(10) Klimov, V.; Mikhailovsky, A.; Xu, S.; Malko, A.; Hollingsworth, J. A.; Leatherdale, C. A.; Eisler, H. J.; Bawendi, M. G. *Science* **2000**, *290*, 314.
(11) Kazes, M.; Lewis, D. Y.; Ebenstein, Y.; Mokari, T.; Banin, U. *Adv. Mater.* **2002**, *14*, 317.
(12) Yin, Y.; Rioux, R. M.; Erdonmez, C. K.; Hughes, S.; Somorjai, G. A.; Alivisatos, A. P. *Science* **2004**, *304*, 711.
(13) Pellegri, N.; Trbojevich, R.; De Sanctis, O.; Kadono, K. *J. Sol-Gel Sci. Technol.* **1997**, *8*, 1023. Martucci, A.; Fick, J.; Schell, J.; Battaglin, G.; Gugliemi, M. *J. Appl. Phys.* **1999**, *86*, 79.
(14) Rogach, A. L.; Nagesha, D.; Ostrander, J. W.; Giersig, M.; Kotov, N. A. *Chem. Mater.* **2000**, *12*, 2676.
(15) Lifshitz, E.; Dag, I.; Litvin, I.; Hodes, G.; Gorer, S.; Reisfeld, R.; Zelner, M.; Minti, H. *Chem. Phys. Lett.* **1998**, *288*, 188.
(16) Mathieu, H.; Richard, T.; Allegre, J.; Lefebvre, P.; Arnaud, G.; Granier, W.; Boudes, L.; Marc, J. L.; Pradel, A.; Ribes, M. *J. Appl. Phys.* **1995**, *77*, 287.

10.1021/cm048477n CCC: $30.25
Published on Web 12/21/2004

hydrophobically modified sol−gel materials (Ormosils) are highly desired since they can naturally entrap the particles without further treatment that could degrade their quality and performance. Indeed, a recent report described the synthesis of hybrid organic−inorganic monoliths doped with core/shell semiconductor NCs, overcoated by hydrophobic surface ligands.[17] The formation of sol−gel glasses doped with semiconductor NCs while maintaining their efficient luminescence using alkylamines as base to catalyze rapid monolithic glass formation was also reported.[18]

We became interested in the entrapment of the NCs within submicrometer hydrophobic/hydrophilic composite sol−gel spheres as a method for protecting the NCs,[19] as a new way for functionalization of silica particles, and as a method for reducing the toxicity of NCs as desired, e.g., in biomedical applications. In this context, we mention that composite sol−gel submicrometer particles made of organic polymers and silica have found applications in catalysis,[20] chromatography,[21] controlled release,[22] and optics[23] and as materials additives (fillers).[24]

The general method we describe here for the entrapment of hydrophobically coated NCs inside micrometer- and submicrometer-sized composite silica spheres is based on earlier work published in this journal.[25] It is a direct one-pot sol−gel preparation procedure of silica−polystyrene (PS) composite particles employing two starting solutions—a hydrophobic solvent containing the sol−gel precursor, the polymer, and the NCs inside and an emulsifying hydrophilic phase which catalyzes the sol−gel polycondenation. The NC entrapment method is demonstrated for a variety of nanocrystals, primarily semiconductors covering different spectral bands, and of different shapes including spheres and rods. We also demonstrate the entrapment of thiol-coated Au particles (useful, for instance, in catalysis[26]), and believe the technique is straightforwardly applicable also for other hydrophobically coated NCs. We term the micrometer-sized particles which contain nanoparticles "nano@micro" composites.

Experimental Details

Chemicals. *Reagents for Nanocrystal Synthesis*. Tri-*n*-butylphosphine (TBP; 99%) and dimethylcadmium ($Cd(CH_3)_2$) were from Strem. $Cd(CH_3)_2$ was vacuum transferred from its original cylinder to remove impurities, and stored in a refrigerator inside a glovebox. Tetradecylphosphonic acid (TDPA) was purchased from Alfa. Hexylphosphonic dichloride ($C_6H_{13}Cl_2PO$; 95%), trioctylphosphine (TOP; 90%; purified by vacuum distillation and kept in the glovebox), trioctylphosphine oxide (TOPO; 90% purity), selenium (Se), indium trichloride ($InCl_3$), hexamethyldisilathiane $\{(TMS)_2S\}$, 1 M diethylzinc $\{Zn(CH_3)_2\}$ in hexane solution, hydrogen tetrachloroaurate trihydrate ($HAuCl_4 \cdot 3H_2O$), 1-dodecanethiol (lauryl mercaptan, $C_{12}H_{25}SH$; 98%), sodium borohydride ($NaBH_4$; 95%), and tetraoctylammonium bromide ($N(C_8H_{17})_4Br$; 98%) were purchased from Aldrich. Tris(trimethylsilyl) arsenide $\{(TMS)_3As\}$ was prepared as detailed in the literature.[27] Hexylphosphonic acid (HPA) was prepared by reacting hexylphosphonic dichloride with water. Solid HPA was then extracted with diethyl ether and isolated by evaporation of the solvent.

Reagents for Composite Sol−Gel Synthesis. Polystyrene, monohydroxy-terminated, MW 10000 (PS-10000), was purchased from Scientific Polymer Products (SP^2). Tetraethoxysilane (TEOS) and Tween 80 (Aldrich Catalog No. 27,436-4) were from Aldrich.

Synthesis of Nanocrystals. All NCs were prepared by known procedures and coated with ligands that render them hydrophobic: CdSe dots,[28] CdSe/ZnS core/shell (CS) dots,[29,30] CdSe rods,[2,31,32] CdSe/ZnS core/shell rods,[33] InAs dots,[34] InAs/ZnSe core/shell dots.[35] These semiconductor nanocrystals are coated by phosphine ligands such as TDP and TOPO, and in the case of rods additionally with phosphonic acids such as TDPA and HPA. Au nanocrystals were also prepared and are coated by 1-dodecanethiol.[36]

Entrapment Procedure of the NCs within the Sol−Gel Composite Spheres. The entrapment procedure is based on the previous procedure published for synthesis of silica−polystyrene composite microspheres.[25] A typical example is given: Two solutions are first prepared: In a 100 mL flask, 12.5 mL of ethanol, 2.5 mL of ammonium hydroxide (25% by volume), and 0.5 mL of the surfactant Tween 80 are mixed. The second solution consists of 1.0 mL of TEOS, various amounts of polystyrene (ranging from 30 to 80 mg), and 1.0 mL of a toluene solution of the coated NCs. Various amounts of NCs were used, ranging from 20 to 60 mg in 1 mL of toluene, depending on the desired concentration. The hydrophobic solution is then added to the hydrophilic solution at once and vigorously stirred overnight. The formed spheres are separated from the solvent by centrifugation for 5 min and then removal of the solvent. For further measurements sonication for 30 min is required to separate the aggregate particles. Table 1 summarizes the various conditions used in the specific cases.

(17) Epifani, M.; Leo, G.; Lomascolo, M.; Vasanelli, L.; Manna, L. *J. Sol-Gel Sci. Technol.* **2003**, *26*, 441−446.
(18) Selvan, T.; Bullen, C.; Ashokkumar, M.; Mulvaney, P. *Adv. Mater.* **2001**, *13*, 985−988.
(19) Correa-Duarte, M. A.; Giersig, M.; Liz-Marzan, L. M. *Chem. Phys. Lett*. **1998**, *286*, 497−501.
(20) Antonietti, M.; Berton, B.; Goltner, C.; Hentze, H. P. *Adv. Mater.* **1998**, *10*, 154; Mecking, S.; Thomann, R. *Adv. Mater.* **2000**, *12*, 953.
(21) Honda, F.; Honda, H.; Koishi, M.; Matsuno, T. *J. Chromatogr*. **1997**, *775*, 13. Bottoli, C. B. G.; Chaudhry, Z. F.; Fonseca, D. A.; Collins, K. E.; Collins, C. H. *J. Chromatogr.* **2002**, *948*, 121. Goworek, J.; Derylo-Marczewska, A.; Stefaniak, W.; Zgrakja, W.; Kusak, R. *Mater. Chem. Phys.* **2002**, *77*, 276.
(22) Velev, O. D.; Furusawa, K.; Nagayama, K. *Langmuir* **1996**, *12*, 2374.
(23) Xu, X.; Friedman, G.; Humfeld, K. D.; Majetich, S. A.; Asher, S. A. *Chem. Mater*. **2001**, *14*, 1249. Lal, M.; Levy, L.; Kim, K. S.; He, G. S.; Wang, X.; Min, Y. H.; Pakatchi, S.; Prasad, P. N. *Chem. Mater*. **2000**, *12*, 2632. Amalvy, J. I.; Percy, M. J.; Armes, S. P. *Langmuir* **2001**, *17*, 4770.
(24) Petrovicova, E.; Knight, R.; Schadler, L. S.; Twardowski, T. E. *J. Appl. Polym. Sci.* **2000**, *77*, 1684−1699. Mousa, W. F.; Kobayashi, M.; Kitamura, Y.; Zeineldin, I. A.; Nakamura, T. J. *Biol. Mater. Res.* **1999**, *47*, 336. Brechet, Y. J.; Cavaille, J. Y.; Chabert, E.; Chazeau, L.; Dendievel, R.; Flandin, L.; Gauthier, C. *Adv. Eng. Mater*. **2001**, *3*, 571−577. Bokobza, L.; Garanaud, G.; Mark, J.; Jethmalani, J. M.; Seabolt, E. E.; Ford, W. T. *Chem. Mater.* **2002**, *14*, 162−167.
(25) Sertchook, H.; Avnir, D. *Chem. Mater.* **2003**, *15*, 1690−1694.
(26) Konya, Z.; Puntes, V. F.; Kiricsi, I.; Zhu, J.; Alivisatos, A. P.; Somorjai, G. A. *Nano Lett.* **2002**, *2*, 907−910.
(27) Becker, G.; Gutekunst, G.; Wessely, H. J. *Z. Anorg. Allg. Chem.* **1980**, *462*, 113−120.
(28) Murray, C. B.; Norris, D. J.; Bawendi, M. G. *J. Am. Chem. Soc.* **1993**, *115*, 8706−8715.
(29) Dabbousi, B. O.; Rodriguez-Viejo, J.; Mikulec, F. V.; Heine, J. R.; Mattoussi, H.; Ober, R.; Jensen, K. F.; Bawendi, M. G. *J. Phys. Chem. B* **1997**, *101*, 9463−9475.
(30) Talapin, D. V.; Rogach, A. L.; Kornowski, A.; Haase, M.; Weller, H. *Nano Lett.* **2001**, *1*, 207−211.
(31) Peng, Z. A.; Peng, X. *J. Am. Chem. Soc.* **2001**, *123*, 1389−1395.
(32) Manna, L.; Scher, E. C.; Alivisatos, A. P. *J. Am. Chem. Soc.* **2000**, *122*, 12700−12706.
(33) Mokari, T.; Banin, U. *Chem. Mater.* **2003**, *15*, 3955.
(34) Guzelian, A. A.; Banin, U.; Kadavanich, A. V.; Peng, X.; Alivisatos, A. P. *Appl. Phys. Lett.* **1996**, *69*, 432.
(35) Cao, Y. W.; Banin, U. *J. Am. Chem. Soc.* **2000**, *122*, 9692.
(36) Brust, M.; Walker, M.; Bethell, D.; Schiffrin, D. J.; Whyman, R. *J. Chem. Soc., Chem. Commun.* **1994**, 801.

Table 1. Entrapment Reaction Conditions for Various Nanocrystals in Silica/Polystyrene Spheres, Forming Nano@micro Particles[a]

	nanocrystal type, size (nm)	NC amt (mg)	PS amt (mg)	size of spheres (nm), figure number
1	CdSe rods, 24.5 × 4.9	20	30	250, Figure 3A
2	CdSe dots, 3.5	40	40	500, Figure 3B
3	CdSe dots, 6	20	50	780, Figure 3C
4	CdSe rods, 11 × 3	30	60	1000, Figure 3D
5	CdSe rods, 15 × 3.8	35	30	300
6	PbSe dots, 10	50	40	500
7	InAs/ZnSe CS, 4.3	20	35	400
8	InAs/ZnSe CS, 6.3	20	35	400
9	Au dots, 6	30	45	750

[a] In all the syntheses described in the table we keep the same parameters for the ethanol, surfactant agent, toluene, TEOS, and ammonium hydroxide; just the PS and NC amounts were changed as shown in the table. The size for dots indicates the average diameter.

Particle Characterization. Low-resolution transmission electron microscopy (TEM) images were obtained using a Phillips Tecnai 12 microscope operated at 100 kV. Low-resolution scanning electron microscopy (SEM) images were taken on an analytical Quanta 200 ESEM microscope of FEI. Samples for TEM were prepared by depositing a drop of ethanol solution with the composite particles onto a copper grid supporting a thin film of either amorphous carbon or carbon/Formvar. The excess liquid was wicked away with filter paper, and the grid was dried in air. Energy-dispersive X-ray spectroscopy (EDS) analyses were conducted on a JEOL-JAX 8600 superprobe. Samples were deposited on a graphite substrate for this analysis. Fluorescence spectra were recorded using a spectrometer/CCD setup (StellarNet model EPP2000). For NC−toluene solutions spectra were taken. For the sol−gel-entrapped NCs, films were prepared from the spheres, after the sol−gel powder was dispersed on the glass substrate, and the emission was detected at a right angle in the detection monochromator, using a photomultiplier tube (PMT). For all fluorescence measurements we used a 473 nm laser line for excitation. Microscopy and fluorescence microscopy images for single nano@micro spheres were measured on a homemade setup described elsewhere.[37] All optical studies were carried out under ambient conditions.

Results and Discussion

1. Overview of the Results. The preparation of various nano@micro particles, where the NCs are rendered hydrophobic by the proper use of ligands, was made possible due to the composite nature of the sol−gel particles: The PS component provides the needed hydrophobic environment for such entrapments, and indeed, this environment proved efficient in entrapment of significantly smaller hydrophobic dyes.[26] We shall see below that the entrapped NCs are not aggregated. Table 1 provides an overview of the nano@micro particles that were prepared, and of the various conditions needed for each case; the generality is clear. As seen in the table, we have focused on a selection of semiconducting nanocrystals that can impart optical functionality to the nano@micro spheres, taking advantage of the widely tunable band gap absorption and emission they exhibit.

2. Entrapment of the Nanocrystals. Following the reaction, the first evidence for entrapment is provided by the color of the sediment containing the composites—which is typical for the specific NC and its size—and the disappearance of that color from the solution. Moving on to TEM, Figure 1A shows a TEM image of CdSe/ZnS core/shell quantum rods with dimensions of 15 × 3.8 nm (length × diameter). Such rods exemplify one of the forms of the highly advanced hydrophobic nanocrystals of interest that can be entrapped by this method. The entrapment can be clearly seen in Figure 1B, where a dotted, single composite sphere with diameter ∼100 nm is shown (sample 5 from Table 1). Note that we do not expect to necessarily resolve elongation of the rods due to the different orientations inside the three-dimensional sphere. Chemical analysis by EDS also provided direct evidence for entrapment. Figure 1C shows the EDS measurement of sol−gel spheres shown in (B): Si from the silica component of the composite, Cd and Se from the nanocrystal core, and Zn and S from the nanocrystal shell were detected. Three composite spheres with nanocrystals encapsulated inside are presented in the inset of Figure 1C. The three-dimensional nature and structure of the spheres, with a diameter of 0.5 μm, is obtained by HRSEM (high-resolution SEM) measured on these samples.

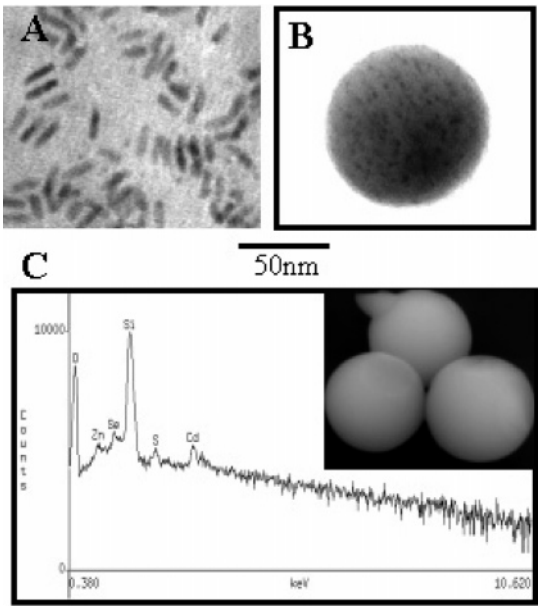

Figure 1. (A) TEM image of CdSe/ZnS core/shell quantum rods (15 × 3.8 nm) that were entrapped in the spheres shown in (B). (B) Nano@micro particle: a composite silica/polystyrene sol−gel particle, ∼100 nm in size, within which the CdSe/ZnS nanorods are entrapped (the nanocrystals are resolved as dark spots). (C) An EDS measurement of the sol−gel spheres with entrapped CdSe/ZnS core/shell nanocrystals. Si, Cd, Se, Zn, and S were detected. The inset shows an HRSEM image of three sol−gel spheres with the nanocrystals inside. The width of the inset is 1.2 μm.

3. Preparation of the Composite Sol−Gel Particles. An issue that presented difficulty in the development of the composite spheres was in the initial yield of well-separated spheres versus connected ones, which form a continuous film. We identified that a critical parameter for aggregation was the PS/TEOS ratio, while the nanocrystal concentration has little effect on such aggregation. The concentration range to obtain a high yield of spheres is about 30−70 mg of PS/mL of TEOS, with the other parameters of all the components the same as described in the Experimental Details for a typical synthesis. We believe that the key was to ensure full entrapment of the PS. An additional source for observed aggregation is fusing after sphere preparation in solution or

(37) Ebenstein, Y.; Mokari, T.; Banin, U. *Appl. Phys. Lett.* **2002**, *80*, 4033.

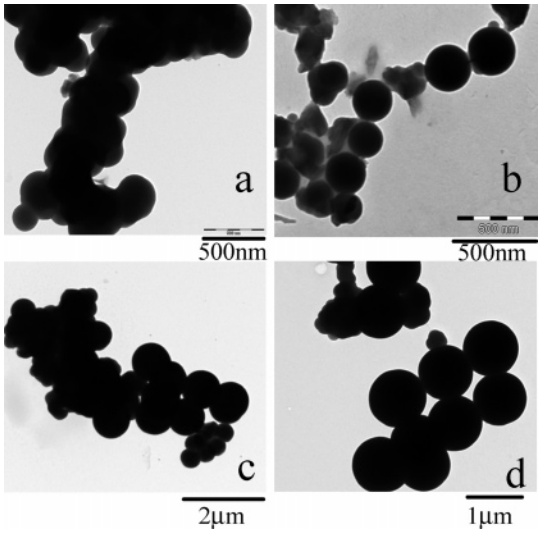

Figure 2. TEM images of the composite sol−gel particles (a) before and (b) after sonication. (c) Spheres on a carbon-coated grid compared with (d) spheres on a carbon/Formvar-coated grid. Entrapped within the spheres are CdSe/ZnS core/shell nanorods of dimensions 15 × 3.8 nm.

directly on the TEM grid, due to strong interparticle interactions. This problem can be minimized, as mentioned in the Experimental Details by sonicating the samples for 1/2 h prior to deposition on the TEM grid (Figure 2a,b), and also by changing the TEM grid surface from carbon-coated to carbon/Formvar-coated grids, which are more hydrophilic, also shown in Figure 2c,d. The latter grid surface attracts more strongly the silica spheres and reduces their mobility once deposited. The process was optimized to the extent that monodisperse silica spheres could be obtained reproducibly (as seen in Figures 1 and 3).

Another important parameter in controlling the nano@micro sphere synthesis is the ability to achieve a narrow size distribution of their size along with size control. Such size control is important for applications such as biolabeling, optical coatings, and optical microcavities.[38] In Figure 3 we demonstrate the ability to control the composite sphere sizes. Four TEM images of sol−gel spheres with nanocrystals encapsulated inside are shown, with diameters ranging from 0.25 to 1 μm (see the Figure 3 caption and Table 1 for more details on these samples). Such size control was achieved mainly by modifying the concentration of the polymer: Increasing its concentration increases the size of the resulting sphere (see Table 1), yet not exceeding the maximal concentration indicated above. Another parameter which is critical for a narrow size distribution is the working pH, that is, the concentration of the sol−gel polycondensation catalyst: it is very critical to work in the pH range of 10.5−11.5 for that purpose. Finally, the reaction time is also an important parameter, which dictates the stability of the particles to high-intensity light or to probing electrons. Optimally, the reaction time should be around 5−7 h.

4. Generality of the Entrapment to Various Nanocrystal Systems and Its Use for Controlling Photoluminescence Properties of the Nano@micro Particles. To further prove the generality of the approach, we entrapped a variety

(38) Cha, J. N.; Bartl, M. H.; Wong, M. S.; Popitsch, A.; Deming, T. J.; Stucky, G. D. *Nano Lett.* **2003**, *3*, 907.

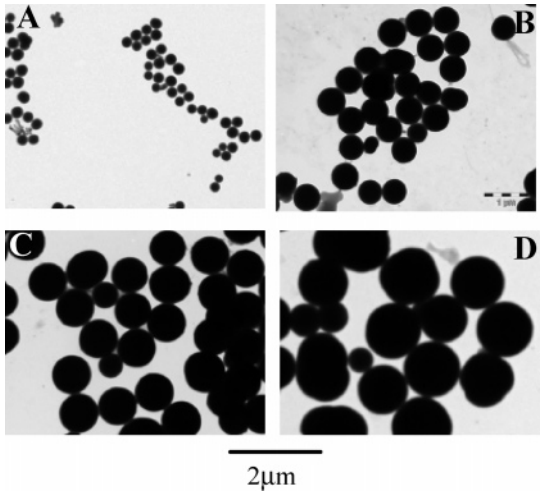

Figure 3. TEM images showing control of the composite particle size: (A) sol−gel spheres (0.25 μm with CdSe/ZnS core/shell nanorods encapsulated inside (dimensions 24.5 × 4.9 nm), (B) sol−gel spheres (0.5 μm) with a CdSe/ZnS core/shell sample (diameter 3.5 nm) encapsulated inside, (C) sol−gel spheres (0.78 μm) with CdSe (diameter 6 nm) nanoparticles encapsulated inside, (D) sol−gel spheres (1 μm) with CdSe/ZnS core/shell nanorods encapsulated inside.

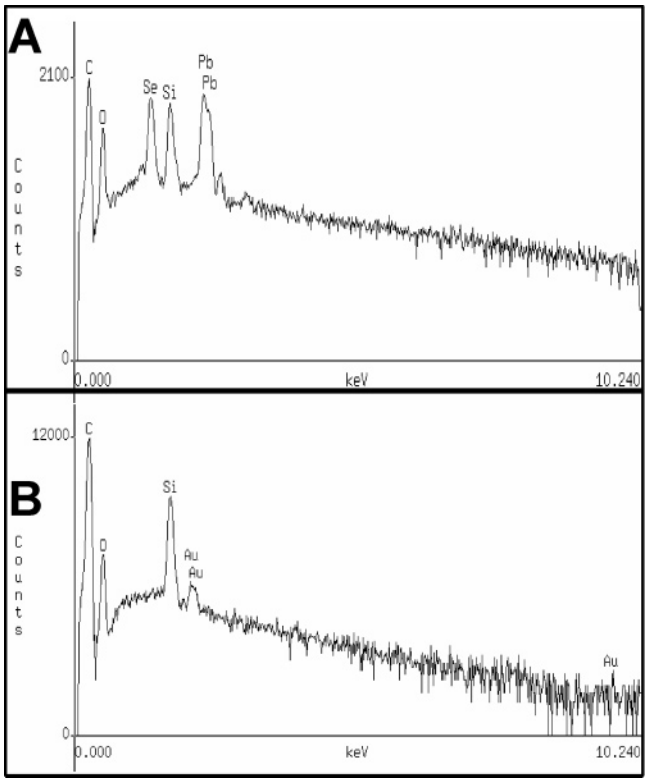

Figure 4. EDS measurements of (A) sol−gel spheres (0.5μm) containing entrapped PbSe nanoparticles (10 nm) (Si, Pb, and Se are seen) and (B) sol−gel spheres (d = 0.75 μm) with entrapped Au nanoparticles (6 nm) (Si and Au are clearly seen).

of semiconductor nanocrystals of various shapes and sizes. For example, we entrapped 10 nm PbSe NCs (Table 1). The EDS spectra of these samples are shown in Figure 4A, and Pb and Se elements are identified. The method is not limited to semiconductor nanocrystals, and we also demonstrated it for thiol-coated Au nanocrystals. Figure 4B also shows the EDS spectra for the Au-encapsulated NCs.

This generality of entrapment can be employed to introduce optical functionality by semiconductor NCs to the

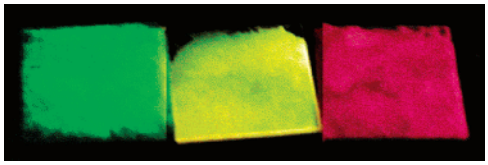

Figure 5. Three films made from composite silica/polystyrene particles within which luminescent CdSe/ZnS core/shell semiconductor nanocrystals are entrapped (green emission, entrapped 11 × 3 nm nanocrystals; yellow, 3.6 nm nanocrystals; red, 25 × 4.5 nm nanorods).

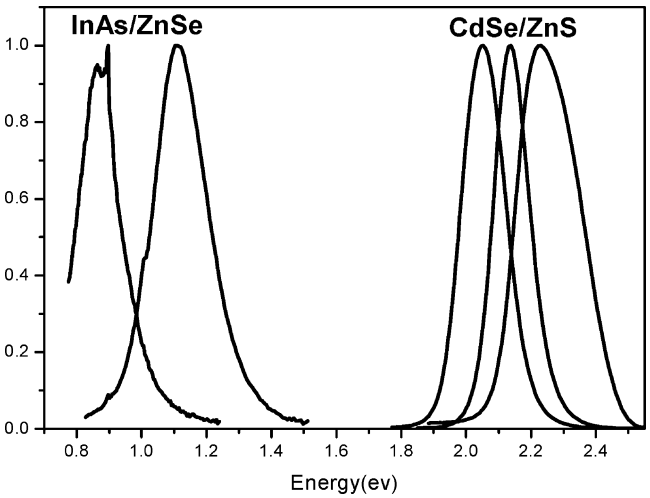

Figure 6. PL spectra of five different nano@micro samples of CdSe/ZnS sol−gel and InAs/ZnSe sol−gel spheres. CdSe/ZnS samples: RS (11 × 3 nm), CS (3.8 nm), RS (25 × 4.5 nm). InAs/ZnSe samples: CS (4.3 nm), CS (6.3 nm). The three films with CdSe/ZnS entrapped are presented in Figure 5. The effect of size on the color of the photoluminescence is directly evident, where green emission was observed for spheres with 11 × 3 nm NCs, yellow for $d = 3.6$ nm NCs, and red for 25 × 4.5 nm NCs.

nano@micro composites. This takes advantage of the wide-range tunable absorption and emission characteristics provided by the unique optical properties of the quantum-confined NCs. Such color-tunable spheres are interesting for various applications as inks, coatings, biomarkers, optical microcavities, and building blocks for photonic band-gap structures. Several types of optical measurements were performed to further verify the entrapment of the nanocrystals in the spheres and to study the effect of entrapment on the photoluminescence. First, visually, the fluorescence of silica spheres containing nanocrystals of various sizes can be seen while the samples are illuminated with a UV lamp. An example is films prepared from the sphere composite silica/polystyrene particles within which luminescent CdSe/ZnS core/shell semiconductor nanocrystals are entrapped as shown in Figure 5.

Even broader spectral coverage can be achieved by encapsulation of semiconductor nanocrystals with different compositions. For instance, InAs-based NCs provide coverage of the near-IR range and were also used in the present study.[35] Figure 6 presents photoluminescence (PL) spectra of three nano@micro sphere samples with CdSe/ZnS NCs that span the visible range from a peak at 556 nm for encapsulated core/shell nanorods of size 11 × 3 nm to 586 nm for core/shell nanodots of diameter 3.8 nm and to a peak of 605 nm for core/shell nanorods of size 25 × 4 nm. Also shown are spectra for samples where two different sizes of InAs/ZnSe NC core/shell nanodots were entrapped, which cover the near-IR range from 1100 nm for core/shell nanodots of diameter 4.3 nm to 1450 nm for core/shell nanodots of diameter 6.3 nm. This directly demonstrates the applicability of our general entrapment method to a variety of semiconductor NCs with different shapes and compositions. We note that the encapsulation leads to a decrease in the fluorescence quantum yield (QY) although quantitative studies were difficult because of scattering of the samples. We found that adding the surfactant, Tween 80, to the NC solution did not quench its fluorescence, while Triton X (used in ref 25) reduced the fluorescence intensity significantly. The observed decrease in the PL of the entrapped NCs is likely due to the effect of exposing the nanocrystals to water in the sol−gel preparation process. The PL of encapsulated nanocrystals is easily observable as shown in Figures 5 and 6. We also note that the PL was still observed even after the nano@micro spheres were left in air for a period of one year.

A more detailed study of the optical properties of the spheres involved a single-sphere analysis with a scanning fluorescence microscope setup, which was also used to provide further direct evidence for the encapsulation of the nanocrystals in the spheres. Figure 7 shows results of this measurement, as follows: Figure 7A shows a far field optical image of three spheres obtained with a digital camera coupled to an inverted microscope with a 100× oil immersion objective under lamp illumination. In Figure 7B we show an image obtained by scanning a sample of spheres deposited onto a microscope coverslip under illumination with an Ar^+ ion laser at 514 nm and an intensity of 1 μW. Two single spheres appear, and on the lower left side of the image an

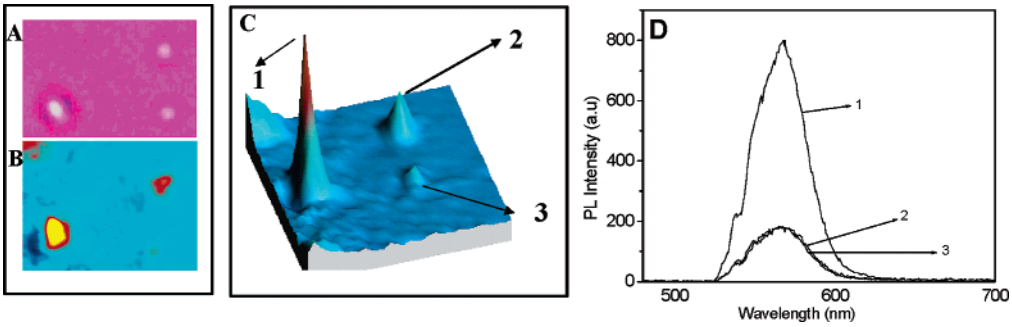

Figure 7. Three composite nano@micro spheres (~500 nm in diameter) containing entrapped core/shell NCs of CdSe/ZnS (3.8 nm), measured by three methods: (A) optical image of the three sol−gel spheres, (B) photon distribution map of the PL emitted by the same spheres, imaged by a scanning fluorescence microscope, **(**C) 3D PL photon distribution maps for the three spheres, measured with a fluorescence microscope setup (the stronger left peak (1) corresponds, most likely, to an aggregate of two composite spheres), (D) corresponding spectra of the three spheres, taken at different integration times (ITs), measured with a fluorescence microscope setup (the stronger left peak corresponds, most likely, to an aggregate of two composite spheres).

aggregate of two spheres can be seen. Three-dimensional PL photon distribution maps for three spheres, collected under 514 nm excitation, and using a long-pass filter to reject the excitation light, are shown in Figure 7B,C. The emission spectrum of the individual spheres was measured by parking the scanning fluorescence microscope on top of each sphere and directing the light to a monochromator−CCD measurement system.

Conclusions

A general method to entrap preprepared hydrophobic nanocrystals into micrometer and submicrometer composite silica spheres was developed. Entrapment of semiconductor nanocrystals imparts optical functionality to the silica spheres, with very broad spectral coverage as dictated by the size, composition, and shape of the entrapped semiconductor nanocrystals. The method could be applied to a variety of semiconductor nanocrystals with sphere or rod shape. The size of the silica spheres can be tuned from about ∼100 nm to several micrometers with good monodispersivity. The method is clearly expanded to encapsulate nanocrystals of metals as demonstrated here for Au. There is no apparent limit to use the principles developed here for encapsulation of any type of hydrophobic nanocrystals of semiconductor, metal, magnetic, or oxide nanocrystals. This directly takes advantage of the significant developments in control of nanocrystals witnessed in recent years, where high-quality particles can be entrapped by a similar approach.

Acknowledgment. This work was supported by the office of the chief scientist of the Israeli Ministry of Commerce and Industry in the framework of the Nano Functional Materials (NFM) consortium. We thank Avi Willenz from the Electron Microscopy Lab of the Life Science Institute for TEM measurements. We thank Mila Palchan from the Unit for Nano Characterization for assistance in the SEM measurements. We are grateful to Nir Tessler from the Technion in Haifa, Israel, for assistance in the fluorescence studies.

CM048477N